The modelling of the Bordoni peak

Gunther Schoeck

The modelling of the Bordoni peak

Journal:	*Philosophical Magazine & Philosophical Magazine Letters*
Manuscript ID:	TPHM-05-Aug-0377.R2
Journal Selection:	Philosophical Magazine
Date Submitted by the Author:	08-Dec-2005
Complete List of Authors:	Schoeck, Gunther; University of Vienna, Institute of Materials Physics
Keywords:	modelling, dislocation mechanics, internal friction
Keywords (user supplied):	

The modelling of the Bordoni peak

by

GUNTHER SCHOECK

Institute of Materials Physics, University of Vienna, Boltzmanng.5,1090 Vienna

E-mail: gunther.schoeck@univie.ac.at

Comment [MK1]: Corrections in redade

Dedicated to Prof. Frank R. N. Nabarro on the occasion of his 90th birthday on March 7,2006

ABSTRACT

In fcc metals kink-pair formation in dislocation lines aligned along close-packed lattice directions can give rise to internal friction effects called Bordoni relaxation. The resulting internal friction peak is a superposition of several individual peaks, each with complex features. In order to study this behaviour, the differential equation describing the movement of dislocation segments by thermally activated kink-pair formation is solved numerically. It is assumed that the kink mobility is high. As result the movement is asymmetric, since the backward movement can occur by kink collapse without need of thermal activation. The influence of the external parameters such as segment length, number of geometrical kinks, internal stress, amplitude and frequency of the applied stress and temperature on the position and shape of the internal friction peaks is studied. When the original configuration is in a bowed out state, the Paré condition is satisfied. Application of an external stress increases the magnitude of internal friction by aligning originally inclined dislocation segments in the direction of the Peierls valleys.

§ 1. Introduction

Straight dislocations lying along close-packed lattice directions have, upon moving, to surmount the ridges of the Peierls-Nabarro potential [1-3]. The crossing of the potential ridges can occur by thermally activated formation of kink-pairs, a process which has been studied in great detail in the literature (for summary see [4–7]).

Thermally activated kink-pair formation in dislocations can give rise to internal friction effects at low temperatures, which in fcc lattices are called Bordoni relaxation There exists a vast literature on the subject and the experimental results have been reviewed by Fantozzi et al. [8] and Richie and Fantozzi [9]. Various attempts have been made to model the mechanism

of the Bordoni relaxation. Esnouf and Fatozzi [10], Schlipf and Schindlmayr [11] and Stadelmann and Benoit [12] considered the occupation probability of various positions of a bowed out dislocation segment and assumed that the transition between neighbouring configurations occurs by kink-pair formation in forward and backward direction. A detailed study of the relaxation process was made by Bujard et al [13], who compared the treatments of the bow-out of a dislocation segment in the string model and the kink-chain model. From their experimental observations using a two-wave acoustic coupling method, they concluded that the results could be explained by a somewhat modified string model. Their experimental results also indicated that the kink mobility in fcc metals is very high, and that in contrast to the Fantozzi-Schlipf-Stadelmann model the annihilation of kink-pairs is not a thermally activated process. Ulfert and Seeger [14] and Seeger [6] derived an analytical expression for the relaxation time from the relaxation function, which is the response to a stepwise increase in applied stress.

We use here a different approach and are going to describe the dislocation behaviour by solving numerically the differential equation for the dislocation velocity under the action of an periodically varying external stress. This will allow to treat a situation, where the forward and backward movement of the dislocations shows different dynamic response and to perform 'numerical experiments', allowing to study the influence of the external parameters like segment length, internal stress, stress amplitude and temperature on the energy dissipation.

§2. The basic assumptions

In order to obtain the rate equation for the dislocation movement we will make the following assumptions:

i) We consider a dislocation segments of length L pinned at the end points either in the same Peierls valley, or n_g valleys of separation a apart with small inclination $g = n_g a/L << 1$. The segment may be subjected to a stress

$$\sigma(t) = \sigma_i + \sigma_0 \sin(2\pi\nu t) \qquad (1)$$

where σ_i is some homogeneous time independent internal or external stress and σ_0 the amplitude of the periodic applied stress.

ii) We will assume that the kink mobility is high, and once a kink-pair has been formed across a saddle point, the kinks will move apart sideways under the action of the applied stress to their equilibrium position in a time small compared to $1/\nu$. This seems be in accordance with experimental observations [13]. Under these conditions the velocity of the dislocation is

controlled by the rate of kink-pair formation Γ per unit length. For a segment of length l moving in the y-direction it is given by

$$\frac{dy}{dt} = alΓ \qquad (2)$$

with kink height *a* [4, 7].

iii) We will assume the final position of the kinks once formed will approximate the configuration of the ideal bow-out in the line tension model. A frictionless dislocation segment of length L running along the x-direction in a single Peierls valley (n_g=0) would, under the action of an applied stress σ, bow-out to a configuration Y(x) which for Y<<L can be approximated by a parabola

$$Y = Y_0\left(1-\frac{4x^2}{L^2}\right) \qquad (3a)$$

with ideal apex height Y_0

$$Y_0(t) = \frac{L^2}{8\gamma}\sigma(t)b \qquad (3b)$$

and with line tension $\gamma = \gamma_0 \mathrm{Log}(R/r_0)$. Here γ_0 is the pre-logarithmic factor of the line tension and R and r_0 of the usual outer and inner somewhat ill defined cut off radii.

When the dislocation movement is controlled by kink-pair formation the instantaneous configuration will be of trapezoidal shape i.e. a parabola truncated by a straight chord at height y (See Fig. 1) and the kinks accumulate at the side branches forming part of the parabola.

[Insert Fig. 1 about here]

iv) Actually not an assumption but rather as result of the high kink mobility, the oscillation of the bow-out is asymmetric. Whereas the forward movement must occur by kink-pair formation, the backward movement under the action of a reverse stress is accomplished by the collapse of kinks, coming from the side branches, without the need of thermal activation.

v) We neglect that in fcc metals dislocations are dissociated into partial dislocations. This can have serious consequences and can lead to multiple equilibrium configurations and the possibility of the formation of fractional kinks [15, 16]. Therefore we may expect that a number of different activation energies can exist and as result a widening of the internal friction peak will occur. The dynamic behaviour of the individual segments will, however, not be affected.

§3. Thermal activation

In trying to derive the formation rate of kink-pairs from the theory of irreversible thermodynamics, we encounter the usual difficulties in treating thermally activated processes. The problem is aggravated by the fact, that we even do not have steady-state conditions. Under the small stresses σ_0 usually employed in internal friction experiments, the saddle point configuration for the formation of kink-pair consists out of two well formed kinks of opposite sign separated by a critical activation distance $d_0 = \sqrt{\gamma_0 a/2\sigma b}$, where *a* is the kink height and b the Burgersvector. The saddle point energy for kink-pair formation is then

$$H_{KP} = 2H_K - \sqrt{2a^3 b\gamma_0\sigma} \qquad (4)$$

where H_K is the energy of an isolated kink [4, 7].

Since typically d_0 is larger than 100 b the formation of the kink-pair by thermal fluctuations must be described by a diffusive drift of the kinks in the interval d_0 across the saddle point [17] and we must apply the diffusion theory of thermal activation. The situation has been discussed in great detail [7, 18] and has been summarised by Seeger [5]. Based on the work of Kramers [19] on diffusion-controlled reactions, he derived for the formation rate Γ of kink-pairs per unit length in an otherwise straight dislocation under the action of a stress σ_{eff}

$$\Gamma = \frac{C_1}{b\sqrt{kT}} F(z) \exp\left[-\frac{2H_K - \sqrt{C_2(\sigma_{eff}/\mu)}}{kT}\right] \qquad (5a)$$

where

$$F(z) = \frac{\sqrt{1+z^2}-1}{z} \qquad (5b)$$

with

$$z = 4\frac{D_K}{kT}\left(2ab^3 m_K^2 \mu^3/\gamma_0\right)^{1/4}\left(\frac{\sigma_{eff}}{\mu}\right)^{3/4} = Z\cdot\left(\frac{\sigma_{eff}}{\mu}\right)^{3/4} \qquad (5c)$$

Here C_1 is a frequency factor which also contains the changes in entropy between the ground state and the saddle point and $C_2 = 2a^3 b\mu\gamma_0$ with shear modulus μ . H_K is the formation enthalpy, D_K the diffusion coefficient and m_K the effective mass of a single kink and kT has its usual meaning. For $z \ll 1$ we have $F(z) = z/2$, however, for $z \to 0$ the theory breaks down [5]. For $z \gg 1$ corresponding to high kink mobilities we have $F(z) = 1$ and the formation rate would formally agree with the one obtained from transition state theory of thermal activation.

The dynamic behaviour is influenced by the magnitude of the dimensionless parameter Z introduced in eq. 5c. Its magnitude is difficult to asset. For the rest mass of the

kink we have $m_K=H_K/c_0^2$ with sound velocity c_0 [5]. For $H_K>>kT$ and for high kink mobility Mann [20] has shown, that agreement with transition state theory can be obtained by setting $D_K = 8w_Kc_0$, where w_K is the kink width. We will use this relation to obtain an order of magnitude estimate of Z. Another estimate for the order of magnitude would be $D_K = \nu_D b^2$ with Debye frequency ν_D. This would lead to a somewhat lower value of Z. With reasonable values for *a* and γ_0 we find from eq. 5c

$$Z \approx 38 \frac{w_K}{b} \frac{\sqrt{H_K \mu b^3}}{kT}. \qquad (6)$$

Introducing the reciprocal temperature $M= T_0/T$ and using as referenced temperature $T_0 = 100$ K, we find from eq 6 with plausible values for the different parameters $Z \approx 2\cdot 10^4$ M but considering the uncertainties involved we will investigate the behaviour over a wide range of Z values.

§4. The dynamic equation for $n_g=0$

We first consider here a simple configuration, where the dislocation segment of length L is anchored in the same Peierls valley, and hence no geometrical but kinks are present ($n_g=0$). The configuration is shown schematically in Fig. 1. When under the action of an external stress $\sigma(t)$ the segment starts to move in the Peierls potential, it will take up the trapezoidal shape of height y (Fig. 1). Due to the bow-out a back stress σ_b will build up and when y(t) reaches ideal apex height $Y_0(t)$ of the frictionless dislocation, the effective stress $\sigma_{eff} = \sigma - \sigma_b$ will vanish. The back stress σ_b will not be homogeneous along the segment length and the largest forward stress exists in the centre of the segment, where kink nucleation will occur preferentially. We can globally take account of this back stress by setting

$$\sigma_{eff} = \sigma\,(Y_0 - y)/Y_0 \qquad (7)$$

Instead of describing the results in terms of the acting stress $\sigma(t)$, it is of advantage in visualizing the results to introduce the ideal apex height $Y_0(t) = L^2 b\sigma(t)/8\gamma$ as variable. With the geometrical relation for the instantaneous segment length $l = L\sqrt{1 - y/Y_0}$ we obtain from eq. 2 for the velocity dy/dt of the chord under the action of a periodically varying stress $\sigma(t)= \sigma_i + \sigma_0 \sin(2\pi\nu t)$ as

$$\frac{dy}{dt} = \frac{C_1}{\sqrt{kT}} \frac{L}{b} \sqrt{1 - \frac{y}{Y_0(t)}} \frac{\sqrt{1+z^2} - 1}{z} \exp\left[-\frac{2H_K}{kT}\right] \exp\left[\frac{b}{L} \frac{\sqrt{C_3 (Y_0(t) - y)}}{kT}\right] \qquad (8a)$$

with $$z = Z\left(\frac{8\gamma}{\mu b L^2}\left(Y_0(t) - y\right)\right)^{3/4} \qquad (8b)$$

and

$$C_3 = 16\, a^3\, \gamma_0\, \gamma / b^2 \qquad (8c)$$

A solution of the highly non-linear differential equation is only possible by numerical methods. When we have determined y(t), we can also obtain the area A(t) swept over by the moving dislocation segment during a cycle. It is given by

$$A(t) = \frac{2}{3}\left(LY_0 - l(Y_0 - y)\right) = \frac{2}{3}LY_0\left(1 - \left(1 - y/Y_0\right)^{3/2}\right) \qquad (9)$$

The energy loss per cycle ΔW is determined by the area of the dynamic hysteresis and hence is given by

$$\Delta W = \oint \sigma(t) b\, dA = \oint b A(t)\, d\sigma = \oint b A(t) \frac{d\sigma}{dt} dt \ . \qquad (10)$$

The internal friction Q^{-1} is defined as the relative energy loss per cycle and given by $Q^{-1}=\Delta W/W$, where $W=\sigma_0^2/2\mu$ is the maximum elastic energy per unit volume stored in the cycle.

§5. Numerical evaluation

For the numerical solution of the differential equation eq. 8 we used a slightly modified version of the standard program of MATEMATICA. For the material parameters we used as typical values $\gamma_0=\mu b^2/(2\pi)$, $\gamma=\mu b^2$, a=b, μb^3 = 4 eV and $2H_K$= 0.15 eV. The constant C_1 was adjusted, that for T–>∞ the frequency of formation f_0 was in the usual range of 10^{10} to 10^{13} sec^{-1} [8]. The value of the parameter Z was varied between 10^3 and 10^7. The frequency ν of the external stress was varied between 1 and 10^9 sec^{-1} and for the amplitude of the applied stress we used the values of $\sigma_0 = 10^{-6}\mu$ and $\sigma_0 = 10^{-5}\mu$. The range of internal stresses investigated was between $\sigma_i = 0$ and $\sigma_i = 10^{-4}\mu$.

§6. The straight segment ($n_g = 0$, $\sigma_i = 0$)

For a straight dislocation segment of length L anchored at each end at points in the same Peierls valley with internal stress $\sigma_i = 0$, the initial condition for the differential equation eq. 8 is y(0) = 0. This is a very special situation, and we only treat it to show, that the kinetic response of a symmetric configuration differs from the one under a bias stress. The numerical solution obtained for $L/b = 10^4$ and $\sigma_0/\mu = 10^{-6}$ is shown in Fig. 2 (lower part) for

[Insert Fig. 2 about here]

values of $M = T_0/T$, for which the energy dissipation is close to the maximum. We show here the applied stress (in units of $10^{-6}\mu$), which is proportional to the back stress of the bow-out with ideal apex height $Y_0(t)$ given by eq. 3b (curve marked Y_0) and a back stress caused by the instantaneous bow-out with height y(t) (curve marked y). For a segment of length L the actual bow-out heights are obtained with the scaling factor $L^2b/8\gamma$.

For t = 0 and when y(t) approaches $Y_0(t)$ the effective stress σ_{eff} of eq. 7 vanishes and hence dy/dt = 0. In the return cycle, when y(t) catches up with $Y_0(t)$, the movement will occur as in a frictionless dislocations, since the kinks can enter from the side branches and collapse. The phase lag between y(t) and $Y_0(t)$) leads to a dynamic hysteresis, which for various values of temperature are shown in Fig 3.

[Insert Fig. 3 about here]

The energy dissipation is proportional to the area of the dynamic hysteresis. For high temperatures it vanishes, because the bow-out approaches the ideal behaviour and for low temperatures it vanishes, because no movement occurs.

We have also studied the influence of the segment length L on the energy loss. The area swept over is proportional to the product Y L and for a fixed stress σ the height Y scales with L^2. Hence the energy loss for a single segment scales with L^3. In order to compare the behaviour for different lengths L, the internal friction peaks shown in Fig. 4 are normalised by L^3. We see

[Insert Fig. 4 about here]

that apart from the difference in height, the peak shape remains the same, but for larger L the peak maximum shifts to smaller values of M (or to higher temperatures). The shift of the reciprocal peak temperature M_0 can be represented by $M_0 = 0.905 - 0.064 \ln(L/b)$. From the shape of a Debye peak, also shown in Fig. 4, it can be seen that the width of each individual peak is about 1.4 larger than the one of a Debye peak. Since a distribution of the segment lengths L would lead to some widening of the total peak, we considered the influence a distribution of segment lengths $N(L)=L/L_0^2 \exp[-L/L_0]$ [21]. The resulting relaxation peak resulting from the superposition showed a width of about 1.6 times of a Debye peak.

§7. The bowed out segment ($n_g=0$, $\sigma_i \neq 0$)

Under the action of a sufficiently high static internal stress σ_i , the dislocations acquires originally a bowed out equilibrium configuration. When we now superimpose a periodically varying stress with amplitude $\sigma_0 < \sigma_i$, the smallest bow-out height occurs at the end of the

backward phase at time $t_0 = 3/(4\nu)$ of the cycle with a stress $\sigma_i - \sigma_0$. The backward movement can occur by kink collapse and hence is in phase with the applied stress. Only when the forward movement starts, kink-pair formation must occur and hence the initial condition for the differential equation eq. 8 is now $y(t_0) = L^2 b(\sigma_i - \sigma_0)/8\gamma$. We note, that at the beginning of the forward movement, the effective length of the segment aligned along the Peierls valley is very small and in the continuum limit we have $l(t_0) = 0$. The segment length will first increase in length by the side movement of the intrinsic kinks on both side arms and decrease when the bow-out height approaches its maximum. The solution of the differential equation when solved for l(t) reproduces exactly these features .

The numerical solution obtained for for $L/b = 10^4$, $\sigma_i/\mu = 2.5\ 10^{-6}$ and $\sigma_0/\mu = 10^{-6}$ is shown in Fig. 2 (upper part). The meaning of the curves Y_0 and y is the same as discussed above. The curve y corresponds to values of $M = T_0/T$, for which the energy dislocation is close to the maximum. The resulting dynamic hysteresis for various values of the temperature are shown in Fig. 5.

[Insert Fig. 5 about here]

The shape of the dynamic hysteresis differs from the one for $\sigma_i = 0$ shown in Fig. 3. This result from the fact, that in the forward cycle, even when the apex at low temperatures cannot bow out due to the lack of kink-pair formation, the existing kinks in the side branches will move apart in phase with the applied stress.

We have also studied the influence of the internal stress σ_i on the shape and the magnitude of the internal friction maxima. The result is shown in Fig. 6 for internal stresses ranging from $1.1\ 10^{-6} \le \sigma_i/\mu \le 10^{-5}$.

[Insert Fig. 6 about here]

When $\sigma_0 > \sigma_i$ the behaviour becomes rather complex and the hysteresis becomes a mixture of the features shown in Fig.3 and Fig.5.

We see that the magnitude of the internal friction peak is largest when the applied stress σ_0 is about of the same magnitude as the internal stress σ_i . In regions with higher internal stress σ_i, the internal friction maximum becomes smaller and shifts to higher temperatures (lower values of M). A distribution of internal stresses therefore can also lead to some widening of the peak. In Fig. 6 we have also shown a superposition of the different peaks, with different values of σ_i together with the shape of an Debye peak. Where as the individual peaks have widths of about 1.4 times the Debye peak, the width of the superimposed peak is 1.6 times as large.

§8. The inclined segment ($n_g>0$)

When a segment of length L anchored at n_g Peierls valley, it will contain n_g geometrical kinks. Its projection on the coordinate x and running along the direction of the Peierls valleys may be L_g. The relaxation function for this configuration has been studied in detail by Seeger [6]. With the origin at the forward anchoring point, the ideal bow-out under the action of a stress σ can be approximated for an original slope $g = n_g a/L_g << 1$

$$Y = (s L_g - g)x - s x^2 \qquad (11)$$

where $s = \sigma b/2\gamma$. For small stresses only the geometrical kinks will move and will be shifted in phase with the applied stress. Kink-pair formation will only become necessary, when the bow-out overshoots the Peierls valley of the forward anchoring point. This will occur at a critical stress $\sigma_{cr} = 2g\gamma/bL_g$, where the tangent to the bow-out that the forward anchoring point is aligned with the directions of the Peierls valley. Simple geometrical considerations show, that for $\sigma > \sigma_{cr}$ the movement can be described by the dynamic equation given by eq. 8with the replacements

$$L \Rightarrow L_g - g/s\,, \qquad Y_0 \Rightarrow Y_g = (s L_g - g)^2/4s, \qquad 1 \Rightarrow L_g\sqrt{1 - y/Y_g} \qquad (12)$$

With these replacements the new dynamic equation has no rational solution, unless the acting stresses σ exceeds the critical stress σ_{cr}. When the static internal stress σ_i is about equal to the critical stress σ_{cr} the internal friction is large. This results from the fact that in this situation a small increase in stress will lead to a large increase in the effective length, where kink-pair formation can take place. When the height of the bow-out overshoots the position of the forward anchoring point, the behaviour becomes more and more similar to the situation with $n_g = 0$ as discussed in the previous section, now however with a variable segment length L. The change of the peak height with increasing σ_i is shown in Fig. 7.

[Insert Fig. 7 about here]

§9. The general segment

Whereas TEM observations in semiconductors or in the bcc metals at low temperature usually show long straight dislocation sections along closed packed directions, no such straight segments were observed in fcc metals. Here dislocations usually form tangles with a wide range of curvature. This is an indication that the Peierls energy and resulting Peierls stress are rather low. It is however important to point out that also such segments can contribute to the Bordoni relaxation. Let us for instance consider a closed dislocation loop, which under the action of internal stress σ_i will take up a shape which can be approximated by

sections of an ellipse elongated in the direction of the Burgersvector. In order to be in stable equilibrium, it must, however, be fixed at two points. When this loop is subjected to a small periodic stress $\sigma_0 << \sigma_i$, it will shrink in the reverse cycle, but in the forward cycle the segments with tangent parallel to close-packed directions can only expand by thermally activated kink-pair formation. This will occur at the apex of the long or short main axis, which are in edge or screw orientation, or in between at segments of 60° or 30° orientation, also along close-packed or second close-packed directions. Their behaviour can formerly be described as in section 7 with $n_g \neq 0$, $\sigma_i \neq 0$.and with length L of the order of magnitude somewhere between the values of the two main axes of the ellipse.

§10. The effective activation energy

When we assume that the formation rate can be expressed by $\nu = \nu_0 \exp[-H_{eff}/kT]$, we can determine the effective activation enthalpy H_{eff} by the shift in peak temperature T with change in frequency ν from

$$H_{eff} = -\frac{d\ln(\nu)}{d(1/kT)} \qquad (13).$$

In our treatment we have assumed $H = 2H_K = 0.15$ eV. From the shift of the peak temperature T_p determined numerically we 'observed' in the frequency range $1 \leq \nu \leq 10^6$ [sec^{-1}] peak temperatures in the range 62 K $\leq T_p \leq$ 125 K and values for the effective activation energy in the range 0.141eV $\leq H_{eff} \leq$ 0.135 eV. The resulting 'experimental' effective activation enthalpy can, within an error limit of $\pm 1 \cdot 10^{-3}$ eV, be represented by

$$H_{eff} = 2H_K - 1.5\ kT \ . \qquad (14)$$

In the range of values of Z given by eq. 5d, we have $F(z) \approx z/2$. We therefore find that the dislocation velocity given by eq. 8 is $\nu \sim (kT)^{-3/2} \exp[-2H_K/kT]$, which, when differentiated, would lead to the result of eq. 14. We see that the agreement with theory and 'numerical experiment' is excellent.

§11.The Paré condition

Considering a straight dislocation segment of length L in a two well potential, Paré [22] pointed out, that when a kink-pair is formed the elastic energy increases by $2H_K$ and that an appreciable interchange of the population between the two configurations can only occur when they have about the same energy. This can be established when the energy difference is compensated by an internal bias stress σ_i satisfying the condition

$$\sigma_i baL = 2\ H_K \qquad (15)$$

In continuum theory (using isothermal elastic constants) the elastic energy is a free energy, where the entropy, resulting from the vibrational lattice modes, is formally represented by the temperature derivative of the shear modulus. But by introducing a kink-pair, the vibrational spectrum of the system is changed and two vibrational modes of the dislocation are replaced by a vibrational and translational mode of the kink-pair. This gives an additional contribution ΔS to the entropy, which in the continuum treatment in eq.15 has not been accounted for. Therefore the right side of eq. 15 should be replaced by $2H_K - T\Delta S$. An estimate of ΔS by Alefeld [23] showed, that the a critical stress σ_i can be reduced considerably.

The situation is however different, when the original configuration is in a bowed out state under the action of an internal stress σ_i. Arsenault [24] and Esnouf and Fatozzi [10] for instance have shown, that there exist, on account of the line tension (or kink-kink interaction), wide shallow potential valleys of the elastic energy, which have an absolute minimum around an equilibrium bow-out height $h_0(\sigma)$ with a number of kink-pairs $n_0(\sigma) = h_0/a$. Bow-outs which differ in height by a single kink-pair have then (due to the mutual elastic interaction) an energy difference much less than $2H_K$. During the forward cycle the number of kink-pairs always is $n(t) < n_0(\sigma)$ and hence the formation of additional kink-pairs is energetically favourable. When in the reverse cycle $n(t)$ catches up with $n_0(\sigma)$, the backward movement will occur by kink-pair collapse in phase with the effective stress, without the need of thermal activation.

The fact, that the height of the Bordoni maximum increases reversibly, when a static external stress is superimposed, has been considered as proof of the Paré concept. As shown above, there is, however, also a different explanation for this stress dependence. Most of the segments in an unstressed sample will be somewhat inclined to the direction of the Peierls valley. They can only participate in the internal friction mechanism, when by an internal (or superimposed external) bias stress they are bowed out to an amplitude, where they start to be lined up with the direction of the Peierls valley.

§12. Discussion

The present approach differs in essential aspects from previous treatments. Paré [22] and Stadelmann and Benoit[12] considered the simple case of a two well potential. Esnouf and Fantozzi [10] (hence EF) and Schlipf and Schindlmayr [11] (hence SS) considered an

ensemble of segments with different number n_i of kink-pairs, where under the action of a varying stress the variation dn_i/dt is established by the formation of kink-pairs in the forward and backward direction from and into the set n_{i-1} and n_{i+1}. This kinetic equation overlooks the fact, that a stable kink-pair cannot be formed in the directions opposite to an acting stress, since no saddle point exists. The treatments further neglect the fact, that the probability of kink-pair formation is proportional to the (variable) chord length l(t). In the treatment of SS it is assumed, that each segment produces a Debye peak, for which the relaxation time depends on the length and the internal stress. Both treatments, as well as an earlier one of Arsenault [24], derived the activation energy for kink-pair formation from the line tension model. Since this is a local approach, it cannot correctly obtain the saddle point energy of kink-pair formation at low stresses, which is not controlled by the crossing of the of the Peierls ridge, but by the long-range interaction to of the two kinks of opposite sign [4, 7]. As result there is in their treatments no direct correlation between the measured effective activation energy (derived from the peak shift) and the energy $2H_K$ of the kink-pair and since the distribution of lengths and σ_i values enters in the exponent, the total internal friction peak obtained by superposition is very wide. In the treatment of Ulfert and Seeger [14] and Seeger [6] the kink-kink interaction is implicitly accounted for. Though postulating a high kink mobility, it is assumed that the velocity of the chord is controlled by the drift velocity of the kinks and the kink concentration ρ_K in thermal equilibrium. Under these conditions the relaxation time for the relaxation function, which is the unidirectional response after a step-wise increase in internal stress, was determined.

A main difference to the previous models results also from the different treatment of the kinetic behavior. In contrast to the assumptions of SS and EF, the kinetics is not described by a periodic disturbance of an equilibrium distribution of kinks, which produce variations in the bow-out heights of the different segments. The energy dissipation rather results from the fact, that in the forward movement each segment lags behind the corresponding equilibrium bow-out. The backward movement, however, occurs by kink-pair collapse in phase with the applied stress.

We have studied here the dynamic behaviour of an individual dislocation segment, by solving numerically the differential equation for its velocity and obtained hereby the correct solution for a system, which satisfies the basic assumption of §2. When we assume that these assumptions apply for the Bordoni relaxation, we can perform 'numerical experiments', by studying the influence of the variations in the external parameters. We can also analyse the situation, where the forward and backward movement is asymmetric, a situation which hardly

could be handled by analytical methods. The solution was obtained under the assumption, that the kink mobility is high and the kinks reach the end of the segment of length L, under the action of an effective stress σ, in a time small compared to the inverse frequency 1/ν. In order that this condition applies, the velocity v_K of the kink must satisfy the condition

$$v_K = \frac{D_K}{kT}\sigma ba \approx \nu_D b \frac{\mu b^3}{kT}\frac{\sigma}{\mu} \geq L\nu \qquad (16)$$

For this estimate we have assumed a temperature-independent diffusion coefficient $D_K = \nu_D b^2$ with Debye frequency ν_D . This seems to be justified for fcc metals, where the kinks are very wide, typically between 15b and 50b [15, 16], and hence can move sideways without the need of thermal activation. With reasonable values for the parameters, the condition of eq. 16 should be generally satisfied, except maybe at extremely low stresses $\sigma/\mu \leq 10^{-8}$ and/or at frequencies in the MHz range.

It is fortunate that for the general features of the internal friction maximum, the details of thermally activated rate process - whether transition state or diffusion theory- is not of major importance. All treatments of the formation of kink-pairs by thermal activation at low stresses contain the exponential term $\exp[-2H_K/kT]$ and the various thermodynamic treatments differ then only in the temperature dependence of the pre-exponential frequency factor. The dynamics of the individual segments is mainly controlled by the instantaneous segment length $l(y,Y_0)$ and the effective stress $\sigma_{eff}(y,Y_0)$, where the ideal apex height Y_0 changes proportional to the applied stress σ. In the Peierls potential the instantaneous chord height y would show a stepwise increase with step height *a*. We used here a continuous function y(t) which somehow averages over segments, and no systematic error is expected from this simplification.

Rather critical for the dynamics is the assumption, that the overall shape of the bow-out (and hence the equilibrium positions of the kinks once formed), is determined by the line tension approach. This would not be expected, when the interaction energy between two kinks of the same sign, separated by a distance r, is given by the asymptotic potential $U = \gamma a^2/2r$, as used in the existing models for kink-chains [13, 23]. This potential is only valid for abrupt kinks and the energy would diverge, when two kinks of opposite sign approach each other. For kinks with finite width the interaction potential between the kinks at close distance is however weaker [25, 26] and when two kinks of opposite sign meet, the energy approaches the one of a kink of twice the height. Since, as discussed above, the kinks in fcc metals are rather wide [15, 16], already for moderate bow-out heights the kinks in the side arms begin to overlap and hence a treatment within the framework of the line tension approach seems to be

appropriate and should describe the typical features. A more detailed realistic treatment of a kink-chain could however, when available, modify the results somewhat.

The internal friction peaks with peak height Q_m^{-1} observed experimentally result of course from a superposition of a large number of individual peaks. With increasing superimposed static stress σ_i the total value of Q_m^{-1} first increases, because more segments a brought in a position to contribute to the internal friction. When however the external stress becomes too large, the internal friction will decrease again, since in highly curved segments the chord length along the Peierls valleys will become smaller. The individual internal friction peaks have a width of about the 1.4 times the width of the Debye peak. When the segment length L increases, the peak temperature T_P increases slightly and the individual peak height q_m^{-1} increases proportional to L^3. When σ_i increases, T_P also increases slightly and q_m^{-1} decreases. A reasonable distribution of each of the parameters L and σ_i would only lead to a moderate widening of about 1.6 times of the Debye peak. Since the width, observed experimentally for the internal friction peaks, is three to four times the Debye width, it is unlikely that it results from a distribution in σ_i and L. It rather will result from a distribution of activation energies. An analysis of the experimental observations, assuming a superposition of Debye peaks to test this assumption, remained inconclusive [27]. A distribution of the formation energy of kink-pairs is, however, to be expected in dissociated dislocations as present in fcc metals. Here the height and profile of the Peierls potential is not unique, but also depends on the (variable) separation of the partial dislocations [15, 16] and a number of metastable equilibrium configurations and fractional kink-pairs can exist.

ACKNOWLEDGEMENT

Stimulating and helpful discussions with Prof. A. Seeger are gratefully acknowledged.

REFRENCES

[1] R. Peierls, Proc, Phys. Soc. London **52**, 34 (1940).

[2] F. R. N. Nabarro, Proc. Phys, Soc, London **59**, 256 ,(1947

[3] F. R. N. Nabarro, Mater. Sci. Eng. A **234,** 67 (1997).

[4] A.Seeger, J. Physique **42** C-5, 201 (1981).

[5] A.Seeger, in: Dislocations 1984, (Veyssière, P.Kubin, J. and Castaign. J. eds) Paris Edition CNRS, pp.141 (1984).

[6] A.Seeger, Mater. Sci. Eng. A **370**, 50 (2004).

[7] J. P. Hirth and J. Lothe, Theory of Dislocations, Wiley, New York (1982).

[8] G. Fantozzi, C. Esnouf, W. Benoit and I. G.Ritchie, Prog. Mater. Sci. **27**, 211 (1982).

[9] I. G. Ritchie and G. Fantozzi, in Dislocations in Solids (F.R.N. Nabarro ed.) North Holland , vol **9,** p 57 (1992).

[10] C. Esnouf and G. Fantozzi, Phys. Stat. Sol. A **47,** 201 (1978) .

[11] J. Schlipf and R. Schindlmayr, Phil. Mag. A**40**, 13 (1979).

[12] P. Stadelmann, and W. Benoit, Helv. Phys. Acta **52**, 637 (1979).

[13] M. Bujard, G. Gremaud and W. Benoit, J. Appl. Phys. **62**, 3173 (1987).

[14] W. Ulfert and A.Seeger, J. de Physique **4,** C8-215 (1996).

[15] G. Schoeck, Phil. Mag. A **82**, 1033 (2002).

[16] G. Schoeck, Phil. Mag. **85**, 949 (2005).

[17] H. Dohnth, Zeitschr. f. Physik **149**, 111 (1957).

[18] A. Seeger and P. Schiller in Physical Acoustics (P. Mason ed.), Academic Press, vol. **III A,** p.361 (1966)

[19] H. A. Kramers, Physica **7**, 284 (1940).

[20] E. Mann, phys. Stat. Sol. B **111,** 541 (1981).

[21] G. Schoeck, Acta Mater. **11**, 617 (1963) .

[22] V. K. Paré, J. Appl. Phys., **32**, 332 (1961).

[23] J. Alefeld, in Lattice Defect and their Interaction (R. R. Hasiguti ed.), Gordon & Breach, New York, p. 408 (1967).

[24] R. J. Arsenault, Acta Metall. **15**, 501 (1967).

[25] A. Seeger and P. Schiller, Acta Met. **10**, 348 (1962).

[26] W. Püschl, G. Schoeck H. O. K. and Kirchner, Phil. Mag **56**, 553 (1987).

[27] D. H. Niblett, J. Appl. Phys., **32**, 895 (1961).

Figure captions.

Fig. 1. Ideal bow-out Y(x) with apex height $Y_0(t)$ and actual bow-out y(t) in the Peierls potential.

Fig. 2. Time dependence of stress σ in units of $10^{-6}\mu$. Curve marked Y_0 is applied stress, which is equal to the back stress of the ideal bow-out Y_0 . Curve marked y is the back stress of the instantaneous bow-out y(t) at a temperature T, where about the maximum energy dissipation occurs. The value of the bow-out for a segment of length L can be obtained by the scaling factor $L^2b/8\gamma$. The acting stress on the moving segment is the difference Y_0-y. Lower curve for $\sigma_i = 0$. Upper curve for $\sigma_i = 3\ 10^{-6}\mu$.

Fig. 3. Dynamic hysteresis for a segment originally along the Peierls valley for various temperatures T:

(1) below the peak temperature T_p, (2) near the peak temperature T_p,

(3) above the temperature T_p .

Fig. 4. Internal friction peaks Q^{-1} (arbitrary units) normalized by L^3 as function of reciprocal temperature for (1) $L= 3\ 10^3b$, (2) $L= 10^4b$, (3) $L= 3\ 10^4b$, with Debye peak D.

Fig. 5. Dynamic hysteresis for a segment with original bow-out due to an internal stress σ_i for various temperatures T:

(1) below the peak temperature T_p, (2) near the peak temperature T_p,

(3) above the temperature T_p .

Fig. 6. Internal friction peaks Q^{-1} (arbitrary units) for a segment of length $L = 10^4b$ as function of reciprocal temperature, for $\sigma_0= 10^{-6}\mu$ and various values of the internal stress σ_i :

(1) $\sigma_i = 1.1\ 10^{-6}\mu$, (2) $\sigma_i = 2.5\ 10^{-6}\mu$, (3) $\sigma_i = 6\ 10^{-6}\mu$, (4) $\sigma_i = 10^{-5}\mu$,

D are Debye peaks, S is superposition of peaks (1) to (4).

Fig. 7. Maximum height of Internal friction peaks Q^{-1} (arbitrary units) for a segment of length $L=10^4b$ inclined to the Peierls valley ($n_g = 50$) as function of ratio σ_i/σ_{cr} . The straight lines connecting the 'measured' points serve only for visualization.

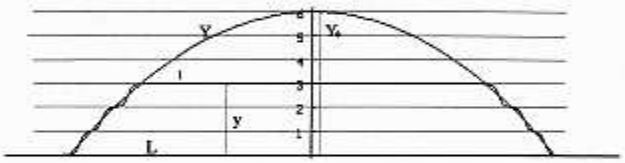

Fig. 1

Figure 1
118x167mm (72 x 72 DPI)

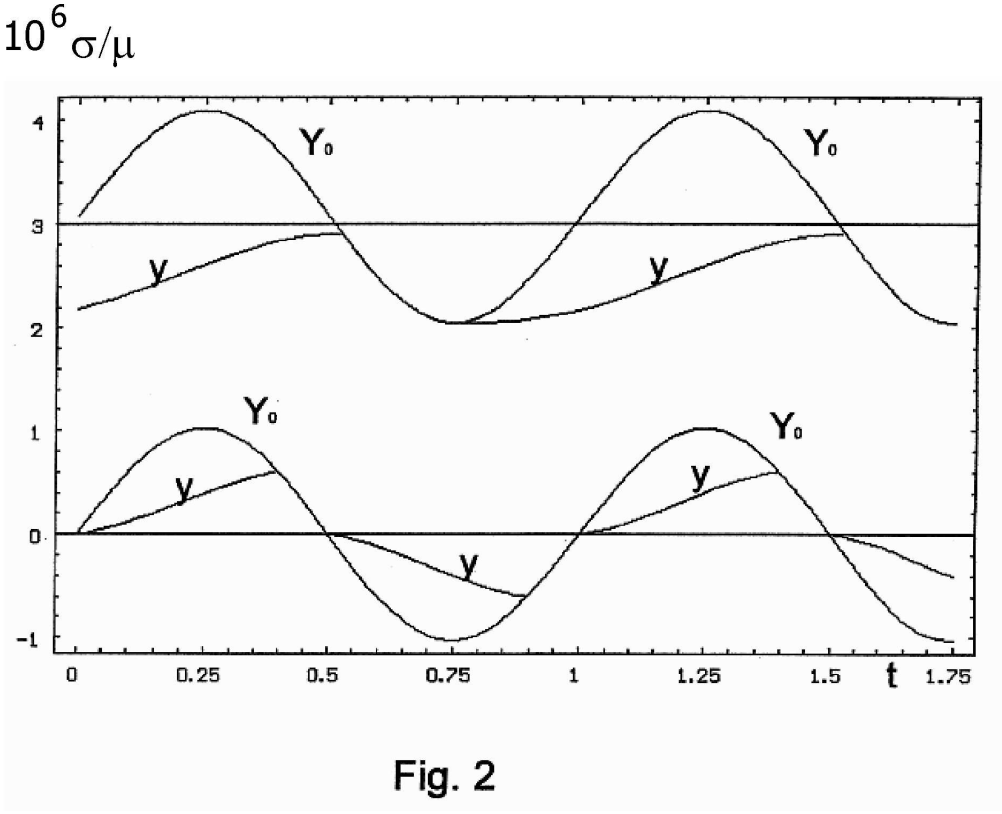

Fig. 2

Figure 2
660x531mm (72 x 72 DPI)

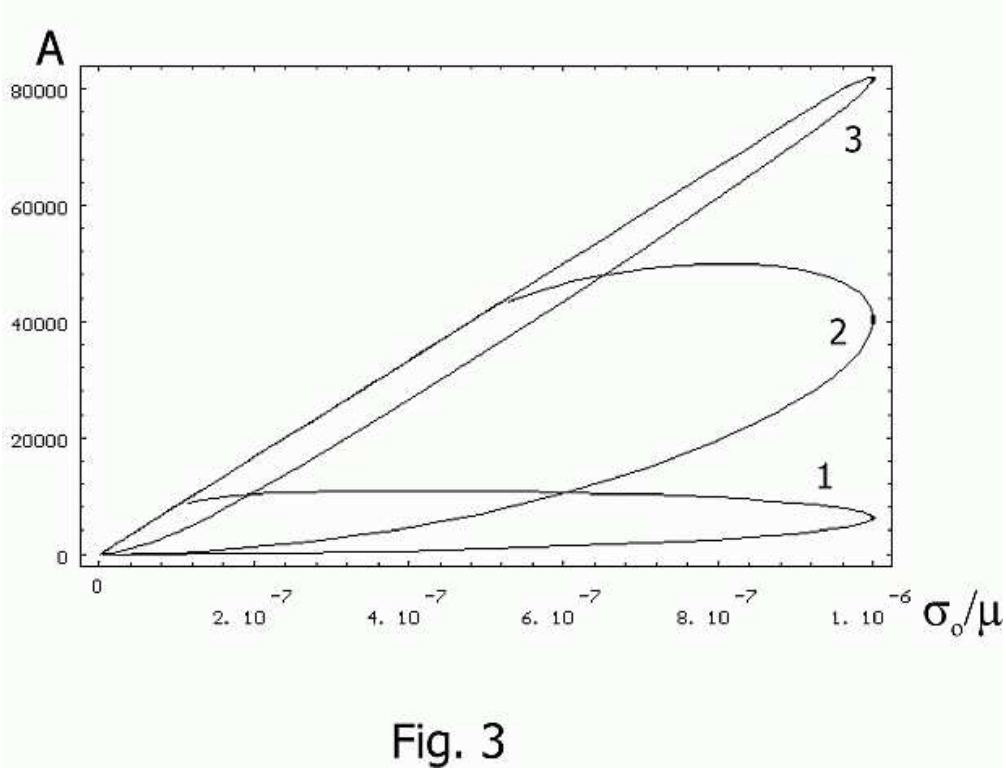

Fig. 3

Figure 3
217x167mm (72 x 72 DPI)

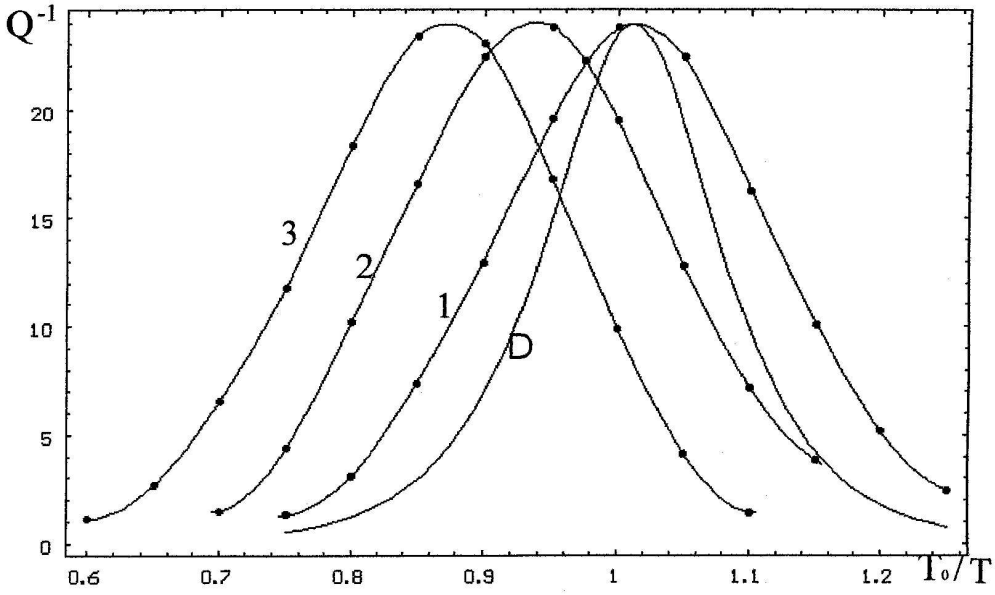

Fig. 4

Figure 4
1716x1173mm (72 x 72 DPI)

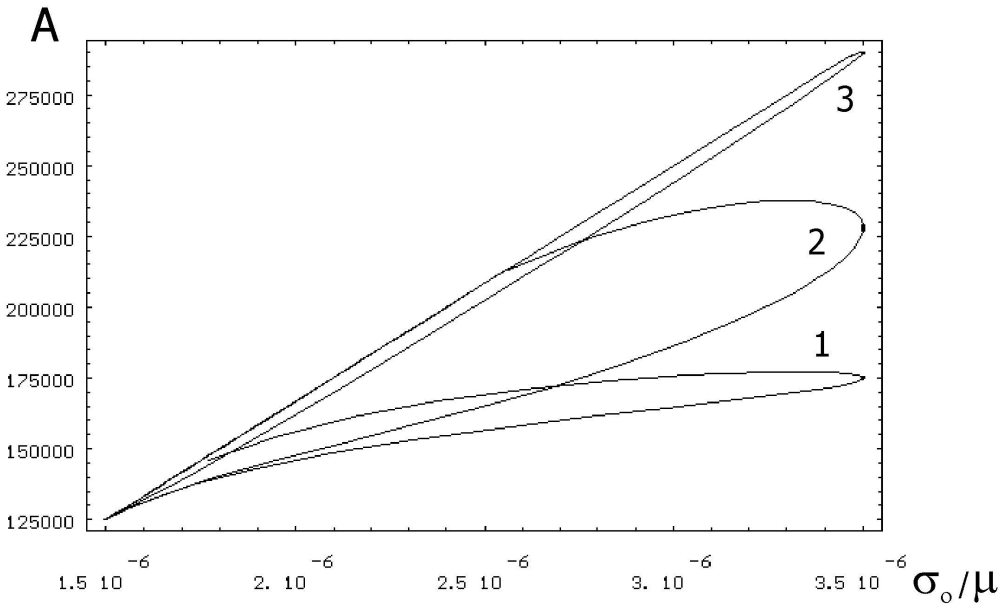

Fig . 5

Figure 5
761x576mm (72 x 72 DPI)

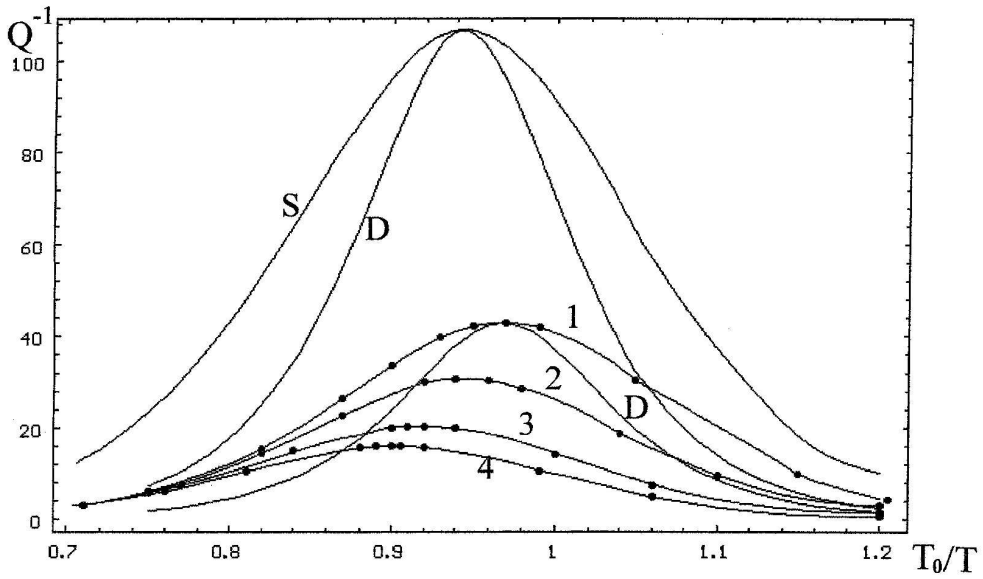

Fig. 6

Figure 6
1738x1126mm (72 x 72 DPI)

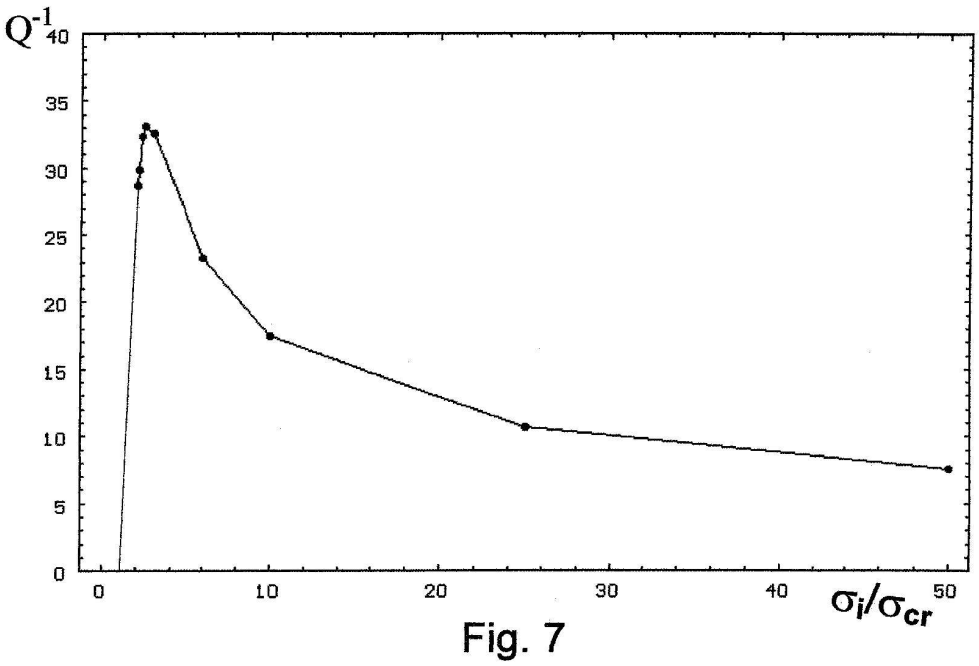

Fig. 7

Figure 7
1733x1185mm (72 x 72 DPI)